

A CONCENTRIC HYDRODYNAMIC JOURNAL BEARING WITH THE BOUNDARY SLIPPAGE

YONGBIN ZHANG

College of Mechanical Engineering, Changzhou University, Changzhou, Jiangsu Province, China
e-mail: engmech1@sina.com

The paper proposes a concentric hydrodynamic journal bearing constructed by the boundary slippage, which is opposed by conventional lubrication theory. Analysis for the carried load and friction coefficient of this bearing is presented. The optimum condition for the maximum load-carrying capacity of this bearing is examined. It is shown that the whole circumference of the bearing should be taken as the lubricated area, while on most of the stationary surface of the bearing there should be a hydrophobic coating covered so that the boundary slippage would occur on this surface. In this condition, the load-carrying capacity of the bearing is the highest but its friction coefficient is the lowest.

Keywords: hydrodynamics, boundary slippage, load, friction, bearing

1. Introduction

Conventional lubrication theory says that no hydrodynamic lubrication effect can be generated between two sliding parallel smooth plane surfaces (Pinkus, 1961). It also denies a concentric hydrodynamic journal bearing, where the lubricating film thickness is circumferentially constant. However, in practice, a concentric hydrodynamic journal bearing is very useful because of its high supporting precision, high lubricating film thickness, low viscous friction and low energy consumption.

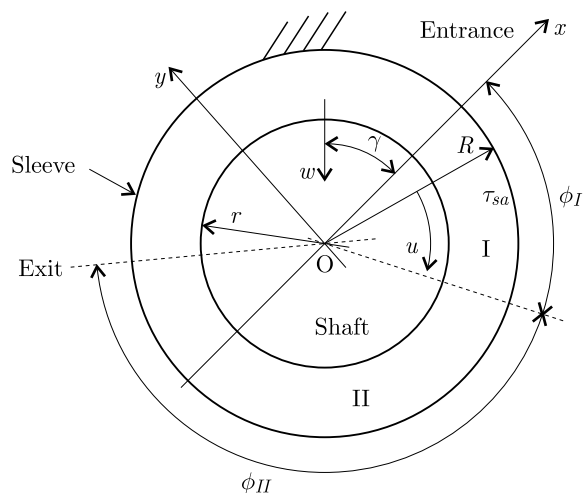
The boundary slippage has been found to be capable of improving the performance of a hydrodynamic lubrication (Salant and Fortier, 2004; Zhang, 2008, 2010, 2013, 2014, 2015b; Li *et al.*, 2014). It was found that hydrodynamic lubrication can be generated between two sliding parallel smooth plane surfaces because of the boundary slippage (Zhang, 2008). While, in conventional bearing configurations, the artificial introduction of the boundary slippage can increase the load-carrying capacity of the bearing but reduce its friction coefficient Zhang (2010, 2013, 2014, 2015b). In Zhang (2015b), the performance of a hydrodynamic journal bearing with an eccentricity was found to be able to be significantly improved by the boundary slippage. However, in that paper, a concentric hydrodynamic journal bearing was not addressed.

This paper proposes a concentric hydrodynamic journal bearing which is formed dependent on the boundary slippage. Analysis of this bearing is presented. It has been found that a significant load-carrying capacity can be generated depending on the design method applied. The optimum condition for the maximum load-carrying capacity of the bearing is also analyzed. In this optimum condition, the bearing also works with the lowest friction coefficient. The study shows a potential application value of such a bearing in practice.

2. The bearing configuration

Figure 1 shows the configuration of the studied bearing. The bearing is formed by a rotating shaft (with circumferential speed u) and a stationary sleeve. The two elements are concentric

and the lubricating film thickness in the bearing is constant and equal to the bearing clearance $c(= R-r)$. The clearance of the bearing is filled with a fluid. The lubricated area of the bearing is divided into two subzones, i.e. "I" and "II" subzones which are, respectively, the inlet and outlet zones of the bearing. On the stationary (sleeve) surface in "I" subzone there is a hydrophobic coating covered to yield a low fluid film-contact surface interfacial shear strength (τ_{sa}) at this surface so that the boundary slippage would occur at this coated surface. The envelope angles of "I" and "II" subzones are respectively ϕ_I and ϕ_{II} . On the other surfaces of the bearing, the fluid film-contact surface interfacial shear strength is relatively high so that the boundary slippage is absent on these surfaces. The radii of the shaft and sleeve are r and R , respectively. The carried load per unit contact width and attitude angle of the bearing are respectively w and γ . The coordinate system used in the analysis is also shown in Fig. 1.



The bearing is filled with a fluid between the shaft and the sleeve. The fluid film slips at the sleeve surface in subzone "II" because of low fluid-sleeve interfacial shear strength τ_{sa} . It does not slip at the other bearing surfaces because of relatively high interfacial shear strength there

Fig. 1. Configuration of the proposed bearing

3. Analysis

The analysis carried out by Zhang (2015b) is also applicable to the present bearing. The analysis is based on the following assumptions:

- The lubricant film thickness is high enough so that the lubricant is continuum across the film thickness;
- The lubricant film is Newtonian within the film;
- The lubricant is isoviscous and incompressible;
- Contact surface deformations are negligible;
- The side leakage in the bearing is negligible and the lubricant is in laminar flow;
- The operating condition is isothermal.

Accordingly to Zhang (2015b), the following dimensionless parameters are defined:

$$W = \frac{wc^2}{u\eta r^2} \quad P = \frac{pc^2}{u\eta r} \quad Q_v = \frac{q_v}{uc} \quad \bar{F}_x = \frac{F_x c^2}{u\eta r^2} \quad \bar{F}_y = \frac{F_y c^2}{u\eta r^2}$$

$$\bar{F}_{f,h} = \frac{F_{f,h}c^2}{u\eta r^2} \quad \bar{F}_{f,s} = \frac{F_{f,s}c^2}{u\eta r^2} \quad \bar{\tau} = \frac{\tau c^2}{u\eta r} \quad k_\tau = \frac{\tau_{sa}c}{u\eta} \quad DU = \frac{\Delta u}{u}$$

Here, η is fluid viscosity, p is film pressure, q_v is volume flow rate in the bearing per unit contact width, F_x and F_y are respectively components of the carried load in the x and y coordinate directions, $F_{f,h}$ and $F_{f,s}$ are respectively friction forces per unit contact width acting on the sleeve and shaft surfaces, τ is shear stress, and Δu is fluid film interfacial slipping velocity.

The pressure boundary conditions in the bearing are:

$$P|_{\phi=0} = 0 \quad P|_{\phi=\phi_I+\phi_{II}} = 0 \tag{3.1}$$

When the eccentricity ratio ε is zero, a lot of the analytical results obtained by Zhang (2015b) are applicable to the present bearing. The following Sections demonstrate those results.

3.1. “I” subzone

The dimensionless Reynolds equation in “I” subzone is:

$$\frac{dP_{slip}}{d\phi} = 3 - 3Q_{v,slip} - \frac{3k_\tau}{2} \tag{3.2}$$

Using the boundary condition in Eq. (3.1), integrating Eq. (3.2) gives dimensionless pressure in “I” subzone:

$$P_{slip} = \left(3 - 3Q_{v,slip} - \frac{3k_\tau}{2}\right)\phi \quad \text{for } 0 \leq \phi \leq \phi_I \tag{3.3}$$

The dimensionless pressure on the boundary between “I” and “II” subzones is:

$$P_{slip,max} = \left(3 - 3Q_{v,slip} - \frac{3k_\tau}{2}\right)\phi_I \tag{3.4}$$

3.2. “II” subzone

The dimensionless Reynolds equation in “II” subzone is:

$$\frac{dP_{slip}}{d\phi} = 6 - 12Q_{v,slip} \tag{3.5}$$

Using the boundary condition in Eq. (3.1), integrating Eq. (3.5) gives dimensionless pressure in “II” subzone:

$$P_{slip} = (6 - 12Q_{v,slip})(\phi - \phi_I - \phi_{II}) \quad \text{for } \phi_I \leq \phi \leq \phi_I + \phi_{II} \tag{3.6}$$

According to Eq. (3.6), the dimensionless pressure on the boundary between “I” and “II” subzones is:

$$P_{slip,max} = (12Q_{v,slip} - 6)\phi_{II} \tag{3.7}$$

Equations (3.3) and (3.6) show that the pressure is respectively linearly distributed in “I” and “II” subzones in the present bearing. Figure 2 schematically shows the pressure distribution in the present bearing.

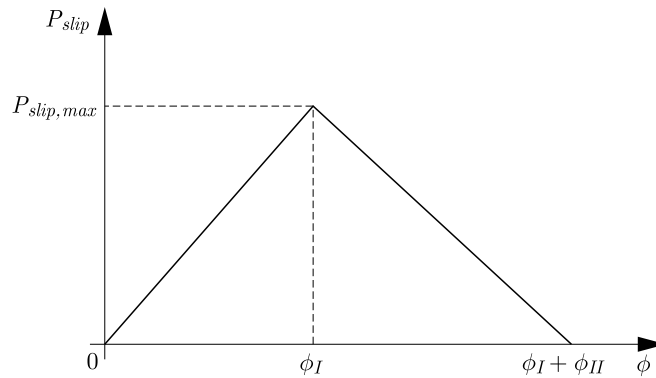


Fig. 2. Illustration of the pressure distribution in the proposed bearing

3.3. Volume flow rate and condition for the bearing

Define $\psi_\phi = \phi_{II}/\phi_I$, solving coupled equations (3.4) and (3.7) gives:

$$Q_{v,slip} = \frac{1 + 2\psi_\phi - \frac{1}{2}k_\tau}{1 + 4\psi_\phi} \quad (3.8)$$

and

$$P_{slip,max} = \bar{P}_{slip,max}(\phi_I + \phi_{II}) \quad (3.9)$$

where $\bar{P}_{slip,max} = 6\psi_\phi(1 - k_\tau)/[(1 + \psi_\phi)(1 + 4\psi_\phi)]$.

From $Q_{v,slip} > 0$, it is obtained that $k_\tau < 2 + 4\psi_\phi$. From $P_{slip,max} > 0$, it is obtained that $k_\tau < 1$. Therefore, $k_\tau < 1$ is the condition for the present bearing.

It is noted from Eq. (3.9) that for given values of k_τ and $\phi_I + \phi_{II}$, when $\psi_\phi = 1/2$, $P_{slip,max}$ reaches the maximum, and its maximum value is $2(1 - k_\tau)(\phi_I + \phi_{II})/3$.

3.4. Carried load and attitude angle of the bearing

The dimensionless hydrodynamic force component in the x axis direction acting on the shaft per unit contact width is:

$$\bar{F}_{x,slip} = - \int_0^{\phi_I + \phi_{II}} P_{slip} \cos \phi \, d\phi = \bar{P}_{slip,max} f_1(\psi_\phi, \phi_{tot}) \quad (3.10)$$

where $\phi_{tot} = \phi_I + \phi_{II}$ and (also Zhang (2015a))

$$f_1(\psi_\phi, \phi_{tot}) = \left(1 + \frac{1}{\psi_\phi}\right) \left[\frac{\psi_\phi \phi_{tot}}{1 + \psi_\phi} \sin\left(\frac{\phi_{tot}}{1 + \psi_\phi}\right) + \cos \phi_{tot} - \cos\left(\frac{\phi_{tot}}{1 + \psi_\phi}\right) \right] \\ - (1 + \psi_\phi) \left[\frac{\phi_{tot} \sin\left(\frac{\phi_{tot}}{1 + \psi_\phi}\right)}{1 + \psi_\phi} + \cos\left(\frac{\phi_{tot}}{1 + \psi_\phi}\right) - 1 \right] \quad (3.11)$$

The dimensionless hydrodynamic force component in the y axis direction acting on the shaft per unit contact width is:

$$\bar{F}_{y,slip} = \int_0^{\phi_I + \phi_{II}} P_{slip} \sin \phi \, d\phi = \bar{P}_{slip,max} f_2(\psi_\phi, \phi_{tot}) \quad (3.12)$$

where (also Zhang (2015a))

$$f_2(\psi_\phi, \phi_{tot}) = \left(1 + \frac{1}{\psi_\phi}\right) \left[\frac{\psi_\phi \phi_{tot}}{1 + \psi_\phi} \cos\left(\frac{\phi_{tot}}{1 + \psi_\phi}\right) - \sin \phi_{tot} + \phi_{tot} \cos \phi_{tot} + \sin\left(\frac{\phi_{tot}}{1 + \psi_\phi}\right) \right] \\ + (1 + \psi_\phi) \left[\sin\left(\frac{\phi_{tot}}{1 + \psi_\phi}\right) - \frac{\phi_{tot}}{1 + \psi_\phi} \cos\left(\frac{\phi_{tot}}{1 + \psi_\phi}\right) \right] \quad (3.13)$$

The dimensionless load per unit contact width carried by the bearing is:

$$W_{slip} = \sqrt{\bar{F}_{x,slip}^2 + \bar{F}_{y,slip}^2} = \bar{P}_{slip,max} f_w(\psi_\phi, \phi_{tot}) \quad (3.14)$$

where $f_w(\psi_\phi, \phi_{tot}) = \sqrt{f_1^2(\psi_\phi, \phi_{tot}) + f_2^2(\psi_\phi, \phi_{tot})}$ (Zhang, 2015a).

Figure 3 plots the values of f_w against ϕ_{tot} for the given values of ψ_ϕ . It is shown that for a given ψ_ϕ , the value of f_w reaches the maximum when $\phi_{tot} = 2\pi$. This means that for the maximum load-carrying capacity of the bearing, ϕ_{tot} should be taken as 2π .

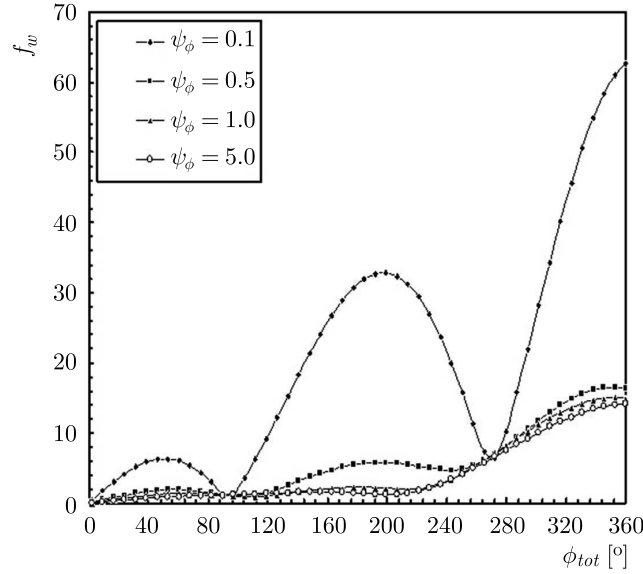


Fig. 3. Plots of f_w against ϕ_{tot} for given ψ_ϕ values (Zhang, 2015a)

When $\phi_{tot} = 2\pi$, the dimensionless load is:

$$W_{slip} = (1 - k_\tau)G(\psi_\phi) \quad (3.15)$$

where $G(\psi_\phi) = 6\psi_\phi f_w(\psi_\phi, 2\pi)/[(1 + \psi_\phi)(1 + 4\psi_\phi)]$.

The attitude angle of the bearing is:

$$\gamma = \arctan \left[\frac{f_2(\psi_\phi, \phi_{tot})}{f_1(\psi_\phi, \phi_{tot})} \right] \quad (3.16)$$

3.5. Friction coefficient and interfacial slipping velocity

The dimensionless shear stress on the shaft surface is:

$$\bar{\tau}_{s,slip} = \begin{cases} \frac{c}{r} \left(3 - \frac{k_\tau}{2} - 3Q_{v,slip}\right) & \text{for } 0 \leq \phi \leq \phi_I \\ \frac{c}{r} (4 - 6Q_{v,slip}) & \text{for } \phi_I < \phi \leq \phi_I + \phi_{II} \end{cases} \quad (3.17)$$

The dimensionless shear stress on the sleeve surface is:

$$\bar{\tau}_{h,slip} = \begin{cases} k_{\tau} \frac{c}{r} & \text{for } 0 \leq \phi \leq \phi_I \\ \frac{c}{r}(6Q_{v,slip} - 2) & \text{for } \phi_I < \phi \leq \phi_I + \phi_{II} \end{cases} \quad (3.18)$$

The dimensionless friction force on the shaft surface per unit contact width is:

$$\begin{aligned} \bar{F}_{f,s,slip} &= \int_0^{\phi_I + \phi_{II}} \bar{\tau}_{s,slip} d\phi = \int_0^{\phi_I} \bar{\tau}_{s,slip} d\phi + \int_{\phi_I}^{\phi_I + \phi_{II}} \bar{\tau}_{s,slip} d\phi \\ &= \frac{c}{r} \left(3 - \frac{k_{\tau}}{2} - 3Q_{v,slip} \right) \phi_I + \frac{c}{r} (4 - 6Q_{v,slip}) \phi_{II} \end{aligned} \quad (3.19)$$

The dimensionless friction force on the sleeve surface per unit contact width is:

$$\begin{aligned} \bar{F}_{f,h,slip} &= \int_0^{\phi_I + \phi_{II}} \bar{\tau}_{h,slip} d\phi = \int_0^{\phi_I} \bar{\tau}_{h,slip} d\phi + \int_{\phi_I}^{\phi_I + \phi_{II}} \bar{\tau}_{h,slip} d\phi \\ &= k_{\tau} \phi_I \frac{c}{r} + \frac{c}{r} (6Q_{v,slip} - 2) \phi_{II} \end{aligned} \quad (3.20)$$

The friction coefficients on the sleeve and shaft surfaces are respectively:

$$f_{h,slip} = \frac{\bar{F}_{f,h,slip}}{W_{slip}} \quad f_{s,slip} = \frac{\bar{F}_{f,s,slip}}{W_{slip}} \quad (3.21)$$

The dimensionless slipping velocity of the fluid film at the sleeve surface is:

$$DU = \begin{cases} \frac{3Q_{v,slip}}{2} - \frac{1}{2} - \frac{k_{\tau}}{4} & \text{for } 0 \leq \phi \leq \phi_I \\ 0 & \text{for } \phi_I < \phi \leq \phi_I + \phi_{II} \end{cases} \quad (3.22)$$

where DU should be positive for $0 \leq \phi \leq \phi_I$.

4. Results and discussion

Figure 4a plots the values of G against ψ_{ϕ} when $\phi_{tot} = 2\pi$. It is shown that G significantly increases with the reduction of ψ_{ϕ} when $\psi_{\phi} \geq 0.1$. While, for $\psi_{\phi} < 0.01$, G is weakly influenced by ψ_{ϕ} . According to Eq. (3.15), it means that for a given k_{τ} the load-carrying capacity of the bearing increases with the reduction of ψ_{ϕ} , especially when $\psi_{\phi} \geq 0.1$, while too low values of ψ_{ϕ} have no benefits in increasing the load-carrying capacity. As the optimum value of ψ_{ϕ} for the maximum value of $P_{slip,max}$ is 0.5, in the engineering design, the value of ψ_{ϕ} may be recommended to be chosen between 0.1 and 0.5.

Figure 4b plots values of γ against ψ_{ϕ} when $\phi_{tot} = 2\pi$. The minimum value of γ is about 57° , and it occurs when ψ_{ϕ} is around 1.0. For $\psi_{\phi} < 0.1$ or $\psi_{\phi} > 20$, γ approaches 90° .

Figures 5a and 5b plot respectively values of $f_{s,slip}r/c$ and $f_{h,slip}r/c$ against ψ_{ϕ} for different k_{τ} when $\phi_{tot} = 2\pi$. It is shown that for given values of k_{τ} and c/r , the friction coefficients $f_{s,slip}$ and $f_{h,slip}$ both are linearly reduced with the reduction of ψ_{ϕ} . This indicates that a relatively low value of ψ_{ϕ} has also benefit of giving a low friction coefficient to the bearing. The reduction of k_{τ} is shown to significantly reduce the friction coefficient, especially when ψ_{ϕ} is high.

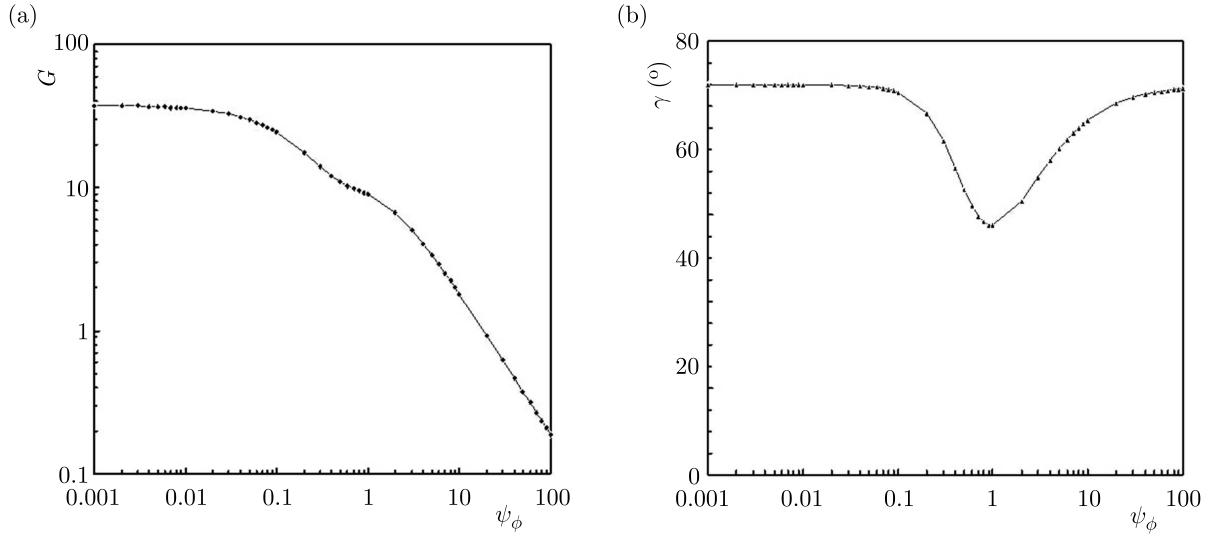


Fig. 4. Plots of (a) G , (b) γ against ψ_ϕ when $\phi_{tot} = 2\pi$

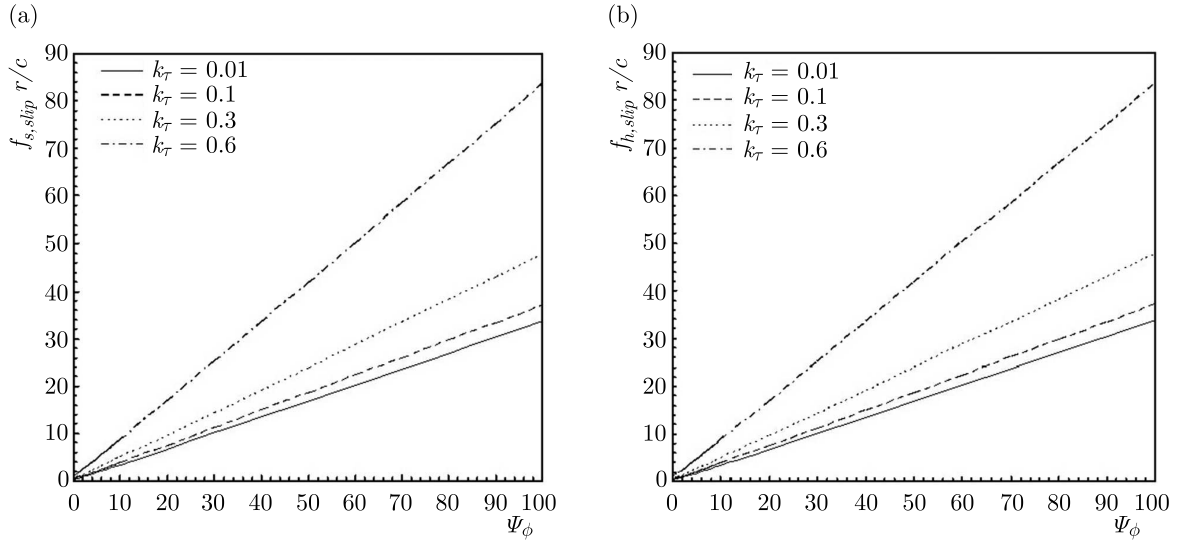


Fig. 5. Plots of $f_{s,slip}r/c$ and $f_{h,slip}r/c$ against ψ_ϕ for different k_τ when $\phi_{tot} = 2\pi$

5. Conclusions

This paper proposes a concentric hydrodynamic journal bearing which is formed dependent on the boundary slippage. The configuration of the bearing is presented. The lubricated area of the bearing is divided into two subzones, which may respectively be the inlet and outlet zones. In the inlet zone, on the stationary surface a hydrophobic coating is covered to yield a low fluid film-contact surface interfacial shear strength so that the boundary slippage could occur on this surface. On the other bearing surfaces, the boundary slippage is absent because of relatively high interfacial shear strengths on these surfaces.

Analysis for the load-carrying capacity and friction coefficient of the bearing is presented. Typical calculations have been carried out. It has been found that the optimum value of the ratio of the circumferential length of the outlet zone to that of the inlet zone, i.e. the optimum value of ψ_ϕ is 0.5 for the maximum hydrodynamic pressure building-up. However for this value ψ_ϕ , the load-carrying capacity of the bearing is still not the maximum. The whole circumference of the bearing should be taken as the lubricated area for achieving a high load-carrying capacity.

In this condition, the carried load of the bearing is found to be increased with the reduction of ψ_ϕ , especially when $\psi_\phi \geq 0.1$. Nevertheless, for $\psi_\phi \leq 0.01$, the load-carrying capacity of the bearing is weakly influenced by variation of ψ_ϕ . It is recommended that in engineering design the value of ψ_ϕ should be chosen between 0.1 and 0.5. A low value of ψ_ϕ also has the benefit of giving a low friction coefficient to the bearing.

References

1. PINKUS O., STERNLICHT B., 1961, *Theory of hydrodynamic lubrication*, McGraw-Hill, New York
2. SALANT R.F., FORTIER A.E., 2004, Numerical analysis of a slider bearing with a heterogeneous slip/no-slip surface, *Tribology Transactions*, **47**, 328-334
3. ZHANG Y.B., 2008, Boundary slippage for generating hydrodynamic load-carrying capacity, *Applied Mathematics and Mechanics*, **29**, 1155-1164
4. ZHANG Y.B., 2010, Boundary slippage for improving the load and friction performance of a step bearing, *Transactions of the Canadian Society for Mechanical Engineering*, **34**, 373-387
5. ZHANG Y.B., 2013, A tilted pad thrust slider bearing improved by boundary slippage, *Meccanica*, **48**, 769-781
6. ZHANG Y.B., 2014, Hydrodynamic lubrication in line contacts improved by the boundary slippage, *Meccanica*, **49**, 503-519
7. ZHANG Y.B., 2015a, A concentric micro/nano journal bearing constructed by physical adsorption, *Journal of the Balkan Tribological Association*, **21**, 937-951
8. ZHANG Y.B., 2015b, An improved hydrodynamic journal bearing with the boundary slippage, *Meccanica*, **50**, 25-38
9. LI G., ZHANG Y.B., JIANG X.D., 2014, A study on the performance of a hydrodynamic step bearing by controlling its boundary slippage in the outlet zone, *Journal of Changzhou University, Natural Sciences Edition*, **26**, 33

Manuscript received April 24, 2015; accepted for print July 29, 2015